Green Chemistry

COMMUNICATION

View Article Online
View Journal | View Issue

Cite this: *Green Chem.*, 2015, **17**, 2745

Received 13th January 2015,
Accepted 16th March 2015

DOI: 10.1039/c5gc00047e

www.rsc.org/greenchem

The use of ultrasonic cavitation for near-surface structuring of robust and low-cost AlNi catalysts for hydrogen production†

P. V. Cherepanov,[a] I. Melnyk,[a] E. V. Skorb,[b] P. Fratzl,[b] E. Zolotoyabko,[c] N. Dubrovinskaia,[d] L. Dubrovinsky,[e] Y. S. Avadhut,[f] J. Senker,[f] L. Leppert,[g] S. Kümmel[g] and D. V. Andreeva*[a]

Ultrasonically induced shock waves stimulate intensive interparticle collisions in suspensions and create large local temperature gradients in AlNi particles. These trigger phase transformations at the surface rather than in the particle interior. We show that ultrasonic processing is an effective approach for developing the desired compositional gradients in nm-thick interfacial regions of metal alloys and formation of effective catalysts toward the hydrogen evolution reaction.

The hydrogen evolution reaction (HER) is an important technological process for the production of molecular hydrogen through water splitting.[1] Catalysts for the HER reversibly bind hydrogen to their surface.[2] Rapid HER kinetics was observed when utilizing expensive metal catalysts.[3–5] Recently, it was shown that near-surface and surface alloys potentially can have excellent catalytic properties for hydrogen production.[6,7] However, up to now such alloys were prepared by time and energy consuming deposition–annealing procedures using transition metals and the Pt(111) surface.[7,8] In this paper, we propose a novel and efficient ultrasound-assisted approach to the manipulation of the metal alloy surface at the atomic level. We use shock impact of billions of collapsing cavitation bubbles during ultrasonic processing for near-surface phase transformation in AlNi particles, the transformation which can hardly be achieved by conventional methods.

According to Nørskov *et al.*,[2] the free energy of hydrogen adsorption (ΔG_{H^*}) on a catalyst surface is a reliable descriptor of catalytic activity for a variety of compounds. The value of ΔG_{H^*} close to zero indicates that hydrogen intermediates are bound neither too strongly nor too weakly to the catalyst surface. In order to disclose which intermetallic phase in AlNi alloys could potentially be active in HER, we calculated the free energy of hydrogen adsorption for AlNi intermetallics (see the ESI† for details of our density functional theory (DFT) calculations).

Fig. 1 demonstrates that the HER can proceed nearly thermo-neutrally at the (100)-planes of Al_3Ni_2. In contrast, a value of ΔG_{H^*} for the Al_3Ni(010) surface plane is more negative due to pronounced surface reconstruction upon hydrogen adsorption and, hence, this plane can be considered equally inactive as pure Ni.

The obtained results, therefore, indicate that the Al_3Ni_2(100) phase in our intermetallic system is expected to be the most active for electrocatalysis. By measuring the particles'

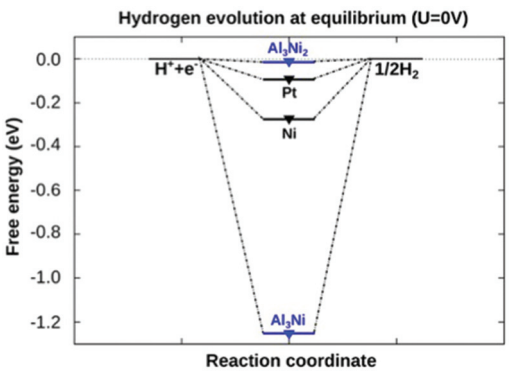

Fig. 1 Calculated free energy diagram for hydrogen evolution at a potential U = 0 relative to the standard hydrogen electrode at pH = 0. Values for Pt and Ni are taken from ref. 33. Al_3Ni_2(100) shows a high potential for the hydrogen evolution reaction.

[a]*Physical Chemistry II, University of Bayreuth, DE-95440 Bayreuth, Germany. E-mail: daria.andreeva@uni-bayreuth.de*
[b]*Max Planck Institute of Colloids and Interfaces, DE-14424 Potsdam, Germany*
[c]*Department of Materials Science and Engineering, Technion – Israel Institute of Technology, 32000 Haifa, Israel*
[d]*Materials Physics and Technology at Extreme Conditions, Laboratory of Crystallography, University of Bayreuth, DE-95440 Bayreuth, Germany*
[e]*Bayrisches Geoinstitut, University of Bayreuth, DE-95440 Bayreuth, Germany*
[f]*Inorganic Chemistry III, University of Bayreuth, DE-95440 Bayreuth, Germany*
[g]*Theoretical Physics IV, University of Bayreuth, DE-95440 Bayreuth, Germany. E-mail: stephan.kuemmel@uni-bayreuth.de*

†Electronic supplementary information (ESI) available: Samples' preparation, PXRD, NMR data, EDS analysis and temperature experiments. See DOI: 10.1039/c5gc00047e

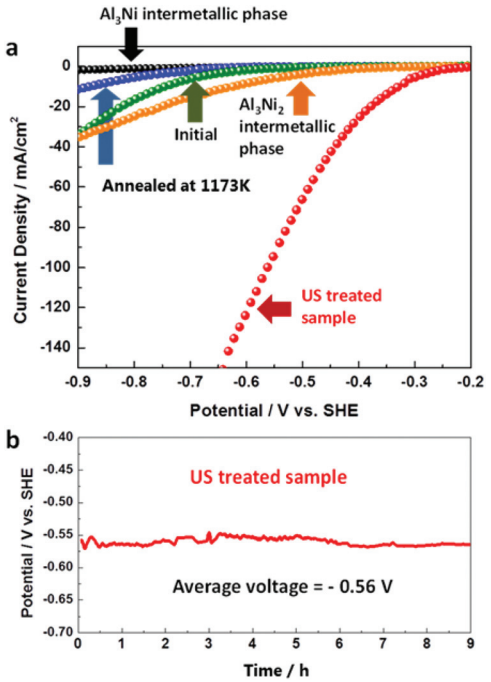

Fig. 2 HER current–potential profiles for the initial and ultrasonically modified AlNi (50 wt% Ni) alloys, bulk commercial Al_3Ni and Al_3Ni_2 phases, as well as AlNi alloy annealed at 1173 K (a). Galvanostatic HER profile for ultrasonically modified AlNi (50 wt% Ni) alloy (b).

activity in HER, we can evaluate how accessible the surface of the $Al_3Ni_2(100)$ phase is for H-adsorption.

In order to experimentally evaluate the predicted activity of the intermetallics during water splitting, we tested the functioning of bulk commercial Al_3Ni_2 and Al_3Ni compounds in HER. The HER current/potential profiles are shown in Fig. 2a.

It is well known that hydrogen production at the surface of efficient electrocatalysts must be characterized with closer to zero overpotential and high current density output. As predicted by our DFT calculations, our experimental results clearly show that the beneficial phase for water splitting is Al_3Ni_2, whereas the Al_3Ni phase binds H too strongly. However, the measured electrocatalytic characteristics of the unstructured bulk Al_3Ni_2 are not as spectacular as predicted by DFT calculations, probably due to the low accessibility of the active $Al_3Ni_2(100)$ planes for hydrogen adsorption. Therefore, the decisive question is whether it is possible to find an efficient method for structuring of the Al_3Ni_2 phase.

Recently, it has been argued that structuring of near-surface regions in metal alloys is of great importance for achieving enhanced catalytic activities of intermetallic compounds.[6] High electrocatalytic activity was observed[7,8] for structured compounds with enhanced accessibility of potentially active crystal planes. Thus, the relatively poor (higher onset overpotential and lower apparent current density values) electrocatalytic behavior of Al_3Ni_2 can be enhanced by structuring of the AlNi alloys containing the Al_3Ni_2 hexagonal phase. Upon controlled structuring of intermetallic phases in the AlNi alloy, we do achieve preferential orientation of the (100) hexagonal crystal planes[9] at the surface and, thus, the enhancement of the Al_3Ni_2 activity toward HER.

According to the AlNi binary phase diagram[10] (Fig. S1, ESI†) and the previous work on electrocatalytic application of AlNi compounds[11–14] the best AlNi candidates for the catalyst preparation are AlNi alloys with nearly 50 wt% of Ni. The Rietveld refinement of the powder X-ray diffraction (PXRD) patterns of the investigated samples showed that this alloy is a mixture of Al (2 wt%), Al_3Ni (43 wt%), and Al_3Ni_2 (55 wt%). However, during alloy preparation from melt, the desirable clustering of Al_3Ni_2 at the surface of Al_3Ni is kinetically restricted due to the preferable nucleation of the Al_3Ni phase on the surface of the already formed Al_3Ni_2 phase. At the same time, the formation enthalpies are $\Delta H \approx -65$ kJ mol^{-1} and $\Delta H \approx -45$ kJ mol^{-1} for Al_3Ni_2 and Al_3Ni, respectively.[15] This means that the Al_3Ni_2 phase is thermodynamically more stable than the Al_3Ni phase. Indeed, according to the equilibrium phase diagram at 1124 K, the Al_3Ni phase can be transformed into the Al_3Ni_2 phase ($Al_3Ni \xrightarrow{1124\ K} Al_3Ni_2 + L_{15.3\ at\%\ Ni}$).[10] Thus, in principle, it should be possible to trigger the desirable phase transformation by conventional heating. However, the obtained product is not electrochemically active (Fig. 2a, blue curve), since the highly active surface planes of the (100)-type remain undeveloped. Therefore, a novel technological solution is required for dedicated near-surface phase transformations in AlNi particles.[16–18]

Technologically fast and controllable local heating of a surface can be achieved by the impact of micron-size high-energy cavitation bubbles.[19] Collapsing of cavitation bubbles that are generated in ethanol by high power ultrasound (HPUS) at 20 kHz induces shock waves and intensive turbulent flow.[20–22] In suspensions cavitation triggers intensive interparticle collisions that result in an extremely rapid local rise of the surface temperature of the sonicated particles followed by quenching down to the surrounding medium temperature of 333 K. In this paper, we investigate the HPUS-induced structuring of the intermetallic phases by using ~140 μm particles of AlNi alloys suspended in ethanol (for details see ESI†). The catalyst preparation route *via* ultrasonication is sketched in Fig. 3 and explained in the ESI,† Fig. S3.

Indeed, the HPUS treatment of AlNi particles causes remarkable modification of the morphology and surface composition in the AlNi alloys. The compositional and morphological changes are clearly visible, when comparing the energy-dispersive X-ray spectroscopy (EDS) results, the ^{27}Al solid state nuclear magnetic resonance (NMR) spectra, X-ray photoelectron spectroscopy (XPS) data and the scanning electron microscopy (SEM) images. The SEM pictures (Fig. 4b) show the surface roughening after the HPUS treatment. This surface modification is clearly revealed in comparison with the relatively smooth particle surface before the treatment (Fig. 4a). Furthermore, EDS analysis of the surface composition of the particles before and after sonication shows a mixture of phases near the surface of pristine particles (Table S2, ESI†). In contrast, after the HPUS treatment (Fig. 4c and d), EDS

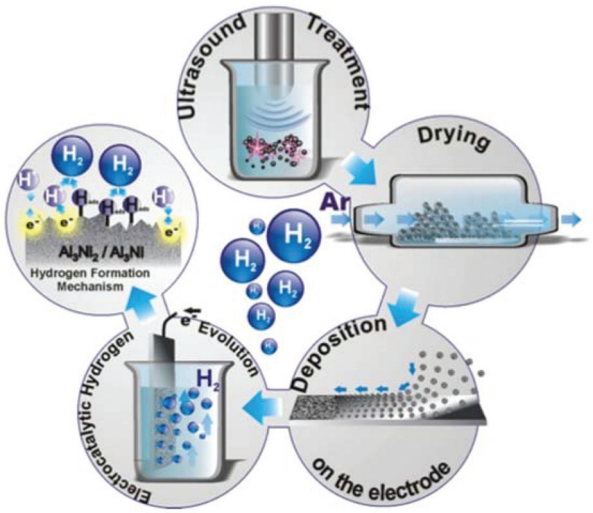

Fig. 3 Schematic illustration of the catalyst preparation procedure. First 10 wt% suspensions of alloy particles (~140 μm) are sonicated in ethanol at a frequency of 20 kHz and an intensity of 140 W cm^{-2} for 1 h. This processing results in the activation of the catalyst surface (change in the crystal structure, phase composition, and morphology). After that the modified particles are centrifuged and dried in an Ar atmosphere. The dried particles are deposited on a substrate and their electrocatalytic activity is evaluated.

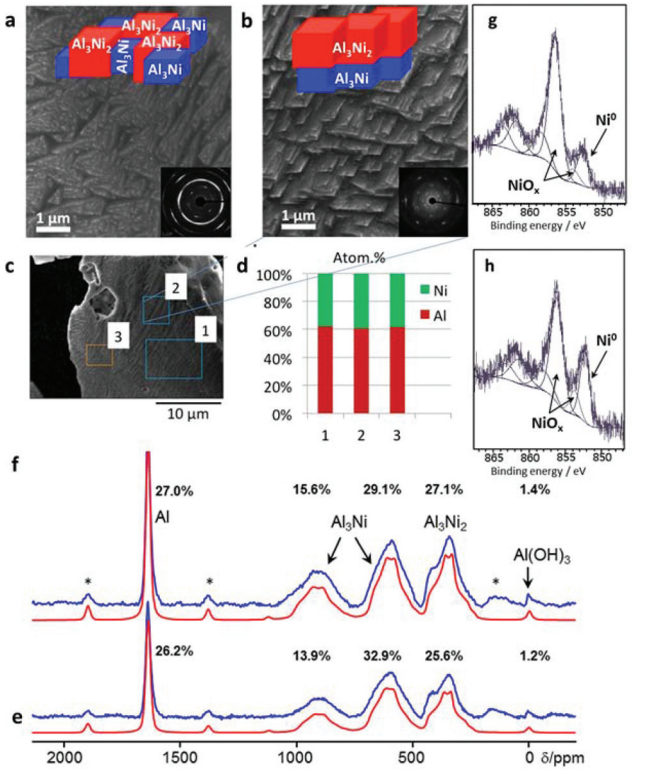

Fig. 4 Scanning electron microscopy images taken from the surface of AlNi (50 wt% Ni) before (a) and after (b) ultrasonication. The inserts show selected area electron diffraction patterns, which demonstrate the tendency to form larger intermetallic crystals after the HPUS treatment. The sketches illustrate the random phase distribution in the initial AlNi particles and the preferential clustering of the Al_3Ni_2 phase upon the HPUS treatment. Energy dispersive X-ray analysis of the metal surface after ultrasonication proves the formation of Al_3Ni_2 at the surface, where aluminum to nickel ratio is 3 : 2 (c, d). ^{27}Al MAS NMR spectra (blue) of the sample sonicated in ethanol (f) as well as pristine AlNi (e) and their corresponding simulated spectra (red) are shown below, respectively. In addition, the relative intensities of each resonance are indicated (see also Table S1, ESI†). The asterisks denote spinning sidebands. X-ray photoelectron spectra of the initial (g) and modified samples (h).

detects the presence of a solitary Al_3Ni_2-phase at the surface. Additional evidence of the microstructure refinement in the alloys after the HPUS treatment is provided by selected area electron diffraction (SAED) (see inserts in Fig. 4a and b). The ultrasonically induced clustering of intermetallic phases in the modified AlNi particles is also schematically illustrated in Fig. 4a and b.

The EDS results, as well as the ^{27}Al solid state NMR spectra (Fig. 4e and f) and XPS surface analysis (Fig. 4g and h), provide clear evidence of the spatial re-distribution of the phases within metallic particles after the treatment.

The EDS results, as well as the ^{27}Al solid state NMR spectra and XPS surface analysis, provide clear evidence of the spatial re-distribution of the phases within metallic particles after the treatment. Due to the skin effect (see ESI†) the penetration depth of rf fields into conducting and magnetic materials is limited. Thus the ^{27}Al NMR spectra (Fig. 4e and f) enhance the surface content of the AlNi alloy before and after ultrasonication. Both materials exhibit five different resonances (Fig. 4e and f) which are assigned on the basis of the observed chemical shift. The main contribution arises from metallic Al (5.7/5.9 wt%), Al_3Ni (52.6/50.1 wt%), Al_3Ni_2 (40.9/43.1 wt%), and $Al(OH)_3$ (0.8/0.9 wt%) before and after sonication. While the Al as well as Al_3Ni ratios are slightly higher compared to the results of the PXRD analysis, the Al_3Ni_2 ratio is lower. This indicates a slight enrichment of Al and Al_3Ni at the surfaces of the alloy particles compared to the bulk composition. Interestingly, sonication increases the surface content of Al_3Ni_2 from 41 to 43 wt%. In parallel the percentage of Al_3Ni decreases from 52.6 to 50.1 wt% leading to a decreased Al_3Ni/Al_3Ni_2 ratio from 1.3 to 1.15. This finding supports the hypothesis that Al_3Ni transforms slowly in Al_3Ni_2 during sonication. In contrast, the PXRD patterns showed that the sonication negligibly affected the bulk ratio of the phases in the samples. Furthermore, XPS surface analysis showed the increased concentration of Ni^0 at the surface (Fig. 4h) upon sonication of AlNi alloy particles in ethanol that also might confirm the formation of the more Ni-enriched Al_3Ni_2 phase compared to Al_3Ni that covers the unmodified surface (Fig. 4g).

The formation of the Al_3Ni_2 phase on the alloy surface is possible if cavitation bubbles can heat the surface to above 1124 K. At this temperature the catalytically inactive Al_3Ni phase is transferred into the beneficial Al_3Ni_2 phase. The spectroscopic surface analysis before and after the HPUS treatment reveals the formation of the Al_3Ni_2 phase and, thus, proves local surface heating up to ~1124 K.

The development of the ultrasonically induced temperature gradient within the particles can stimulate additional crystal growth. We analyzed the PXRD patterns (Fig. S4, ESI†) and calculated the crystallite sizes before and after the HPUS treatment using the Williamson–Hall (W–H) method[23–25] (for details, see ESI†). According to our estimations, the Al_3Ni_2 and Al_3Ni crystallites in the HPUS-treated AlNi are nearly twice as large (131 nm for Al_3Ni_2; 113 nm for Al_3Ni) as pristine particles (87 nm for Al_3Ni_2; 56 nm for Al_3Ni). By assuming diffusion-controlled crystal growth during the treatment period (1 h), we estimate the diffusion rate in the AlNi (50 wt% of Ni) to be about 2×10^{-18} m^2 s^{-1}. The reference experiments (heating the particles in an oven for 1 h at different temperatures (for details see Fig. S5, ESI†)) showed that the observed atomic diffusion proceeds at an average temperature in the particle interior that is about $T \approx 823$ K.

Surface structuring *via* ultrasonication increases the accessibility of the DFT-predicted beneficial $Al_3Ni_2(100)$ phase for H adsorption, which in turn should enhance the catalytic efficiency toward HER. In fact, we did observe outstanding improvement of the electrocatalytic properties (Fig. 2a) of AlNi particles after ultrasonication. The onset overpotential *vs.* SHE is significantly lowered to −0.25 V as compared to −0.65 V for pristine AlNi alloy particles. At the same time, the apparent current density values are strongly enhanced. For example, a drastic (more than 200-fold) increase in the current density was observed at an onset overpotential value of −0.4 V and was found to be 28.19 mA cm^{-2} (HPUS-treated) as compared to 0.13 mA cm^{-2} (initial).

Another very important parameter for evaluating the material's electrocatalytic performance is the exchange current density (i0), which reflects the intrinsic rate of electron transfer between the electrocatalyst's surface and the analyte. Therefore, we replotted the HER current/potential profiles in the Tafel coordinates and calculated i0-values for both the pristine and the HPUS-treated AlNi alloy particles. The calculated i0-value of 17.37 mA cm^{-2} for the HPUS-modified alloy particles is three orders of magnitude higher than for the untreated ones (0.016 mA cm^{-2}). All in all, our study shows that HPUS is a unique technological approach for producing the low-cost and efficient AlNi catalyst for water splitting. The ultrasonically generated AlNi catalyst is very robust and exhibits excellent stability in electrochemical use (Fig. 2b).

Conclusions

Using density functional theory, we first predicted that the Al_3Ni_2 phase is potentially effective in the hydrogen evolution reaction. However, bulk unstructured Al_3Ni_2 compounds demonstrated relatively low efficiency due to the low accessibility of the favorable (100) atomic plane. We propose structuring of AlNi alloys containing the Al_3Ni_2 phase as an efficient and low cost technological approach for enhancing the accessibility of the $Al_3Ni_2(100)$ planes that are active in hydrogen adsorption. The formation of the Al_3Ni_2 phase on the surface of AlNi alloys is kinetically restricted, but we demonstrate that processing of the metal surface by ultrasonically generated cavitation bubbles creates large local temperature gradients in the metal particles. These stimulate the desired phase transformations at the surface rather than in the particle interior. In particular, we show that collapsing cavitation bubbles heat the surface above 1124 K, thus triggering the near-surface transformation of the catalytically inactive Al_3Ni phase into beneficial Al_3Ni_2. In the particle interior, the estimated mean temperature reaches 824 K, which is well below the phase transition temperature, but still enough for substantial solid-state diffusion and crystal growth. This simple, fast, and effective ultrasonic approach toward directed surface modification can be extended to other intermetallic systems for sustainable energy generation.

Experimental

The AlNi (50 wt% Ni) alloy was prepared by melting Al (99.99% purity grade) and nickel (99.99% purity grade) foils (purchased from Sigma-Aldrich) using a Mini ARC melting device MAM-1 (Edmund Bühler Gmbh), TIG 180 DC. The HPUS treatment of AlNi alloy particles was performed using a Hielscher UIP1000hd, (Hielscher Ultrasonics GmbH, Germany) at an operating frequency of 20 kHz. Electrochemical characterization was accomplished in a three electrode cell using a 510 V10 Potentiostat/Galvanostat in the 1 M H_2SO_4 electrolyte. PXRD accompanied by Rietveld refinement, SEM and energy-dispersive EDS and solid state ^{27}Al NMR[26] were employed to verify the phase composition of the prepared AlNi alloys. TEM was used to obtain SAED patterns. DFT calculations were performed using the Vienna ab-initio Simulation Package.[27–32] Detailed information regarding sample preparation, ultrasound treatment, characterization methods, and calculations is available in the ESI.†

Acknowledgements

This work was financially supported by the A11, B1 and C1 projects of SFB 840. The authors thank Dr Beate Förster and Martina Heider (University of Bayreuth) for the SEM and EDS measurements, Carmen Kunnert for the TEM and ED measurements, Sebastian Koch, Bernd Putz, and Dr Wolfgang Millius (Inorganic Chemistry I, University of Bayreuth) for assistance with XRD measurements, and Katharina Schiller, Matthias Daab and Anna Kollath for help with samples' preparation.

Notes and references

1 A. Züttel, A. Borgschulte and L. Schlapbach, *Hydrogen as a future energy carrier*, Wiley-VCH, Weinheim, Germany, 2008.

2 E. Skulason, V. Tripkovic, M. E. Björketun, S. Gudmundsdottir, G. Karlberg, J. Rossmeisl, T. Bligaard, H. Jonsson and J. K. Nørskov, *J. Phys. Chem. C*, 2010, **114**, 18182.
3 B. Hinnemann, P. G. Moses, J. Bonde, K. P. Jorgensen, J. H. Nielsen, S. Horch, I. Chorkendorff and J. K. Nørskov, *J. Am. Chem. Soc.*, 2005, **127**, 5308.
4 T. F. Jaramillo, K. P. Jørgensen, J. Bonde, J. H. Nielsen, S. Horch and I. Chorkendorff, *Science*, 2007, **317**, 100.
5 M. S. Faber and S. Jin, *Energy Environ. Sci.*, 2014, **7**, 3519.
6 J. Greeley and M. Mavrikakis, *Nat. Mater.*, 2004, **3**, 810.
7 A. S. Bandarenka, A. S. Valera, M. Karamad, F. Calle-Vallejo, L. Bech, F. J. Perez-Alonso, J. Rossmeisl, I. E. L. Stephens and I. Cherkendorff, *Angew. Chem., Int. Ed.*, 2012, **51**, 11845.
8 J. Knudsen, A. U. Nilekar, R. T. Vang, J. Schnadt, E. D. L. Kunkes, J. A. Dumesic, M. Mavrikakis and F. Nesenbacher, *J. Am. Chem. Soc.*, 2007, **129**, 6485.
9 P. V. Cherepanov, I. Melnyk and D. V. Andreeva, *Ultrason. Sonochem.*, 2015, **23**, 26.
10 D. Batalu, G. Cosmeliata and A. Aloman, *Metal. Int.*, 2006, **11**, 36.
11 P. V. Cherepanov, M. Ashokkumar and D. V. Andreeva, *Ultrason. Sonochem.*, 2015, **23**, 142.
12 D. Miousse and A. Lasia, *J. Appl. Electrochem.*, 1995, **25**, 592.
13 P. Los, A. Rami and A. Lasia, *J. Appl. Electrochem.*, 1993, **23**, 135.
14 A. Rami and A. Lasia, *J. Appl. Electrochem.*, 1992, **22**, 376.
15 D. Shi, B. Wen, R. Melnik, S. Yao and T. Li, *J. Solid State Chem.*, 2009, **182**, 2664.
16 A. Ilbagi, P. D. Khatibi, H. Henein, R. Lengsdorf and D. M. Herlach, *J. Phys.: Conf. Ser.*, 2011, **327**, 1.
17 D. M. Herlach, *Phase transformation in multicomponent melts*, John Wiley & Sons Ltd, 2009.
18 J. Dulle, S. Nemeth, E. V. Skorb, T. Irrgang, J. Senker, R. Kempe, A. Fery and D. V. Andreeva, *Adv. Funct. Mater.*, 2012, **22**, 3128.
19 B. J. H. Bang and K. S. Suslick, *Adv. Mater.*, 2010, **22**, 1039.
20 K. S. Suslick, *Science*, 1990, **247**, 1939.
21 S. J. Doktycz and K. S. Suslick, *Science*, 1990, **247**, 1067.
22 W. B. McNamara, Y. T. Didenko and K. S. Suslick, *Nature*, 1999, **401**, 772.
23 T. Ungar, A. Revesz and A. Borbely, *J. Appl. Crystallogr.*, 1998, **31**, 554.
24 K. Venkateswarlu, A. C. Bose and N. Rameshbabu, *Physica B*, 2010, **405**, 4256.
25 A. K. Zak, W. H. A. Majid, M. E. Abrishami and R. Yousefi, *Solid State Sci.*, 2011, **13**, 251.
26 R. Bhattacharyya, B. Key, H. Chen, A. S. Best, A. F. Hollenkamp and C. P. Grey, *Nat. Mater.*, 2010, **9**, 504.
27 G. Kresse and J. Furthmüller, *Comput. Mater. Sci.*, 1990, **6**, 15.
28 G. Kresse and J. Furthmüller, *Phys. Rev. B: Condens. Matter*, 1996, **54**, 11169.
29 P. E. Blöchl, *Phys. Rev. B: Condens. Matter*, 1994, **50**, 17953.
30 J. K. Nørskov, T. Bligaard, A. Logadottir, J. R. Kitchin, J. G. Chen, S. Pandelov and U. Stimming, *J. Electrochem. Soc.*, 2005, **152**, J23.
31 H. J. Monkhorst and J. D. Pack, *Phys. Rev. B: Solid State*, 1976, **13**, 5188.
32 B. Hammer, L. B. Hansen and J. K. Nørskov, *Phys. Rev. B: Condens. Matter*, 1999, **46**, 7413.
33 J. Greeley, T. F. Jaramillo, J. Bonde, I. B. Chorkendorff and J. K. Nørskov, *Nat. Mater.*, 2006, **5**, 909.